

Self-Assembly of Poly(1,1-diethylsilabutane)-*block*-poly(2-hydroxyethyl methacrylate) Block Copolymer. 1. Micelle Formation and Micelle–Unimer–Reversed Micelle Transition by Solvent Composition

Minoru Nakano, Masaki Deguchi, Kozo Matsumoto, Hideki Matsuoka, and Hitoshi Yamaoka*

Department of Polymer Chemistry, Kyoto University, Kyoto 606-8501, Japan

Received December 11, 1998; Revised Manuscript Received July 13, 1999

ABSTRACT: Amphiphilic block copolymer poly(1,1-diethylsilabutane)-*block*-poly(2-hydroxyethyl methacrylate) (poly(SB-*b*-HEMA)) was synthesized by addition of 2-(*tert*-butyldimethylsiloxy)ethyl methacrylate to a living poly(1,1-diethylsilabutane) end-capped with 1,1-diphenylethylene and subsequent hydrolysis of silyl-protecting groups. These copolymers formed spherical micelles in methanol. Small-angle X-ray scattering (SAXS) measurements revealed that the aggregation number of the micelle strongly depends on the polymer composition, while total micellar size is almost independent of the degree of polymerization of HEMA. SAXS measurements were also performed for the polymer with the highest degree of polymerization of SB in methanol/toluene mixed solvents. The polymer in the solution was found to have different morphology depending on the mixing ratio of the solvent; i.e., micelle–unimer–reversed micelle transition with increasing toluene content was clearly observed.

I. Introduction

Block copolymers self-assemble in selective solvents. They form micelles in bulk consisting of an inner core composed of solely insoluble segments and an outer shell of soluble segments swollen by the solvent. They are also adsorbed at the surface when insoluble segments favorably interact to the surface. Many groups have studied these specific behaviors of amphiphilic polymers during the past few decades.^{1–4} Amphiphilic copolymers are important materials in the fields of natural science, such as colloid science and biochemistry, as well as in industrial fields. There are a variety of applications of them such as emulsifier, colloid stabilizer, drug delivery systems, and so on. The physicochemical understanding of the block copolymer/solvent system, in particular, investigation of the relationship between block copolymer composition and aggregation state, is important and demanded for these applications.

Copolymers with narrow molecular weight distribution (MWD) must be obtained to analyze the properties of their self-assembly systems. We have been trying to create novel amphiphilic polymers with narrow MWD and investigate their properties.^{5–8} Previously, we have reported the living anionic ring-opening polymerization of 1,1-diethylsilacyclobutane and block polymerization with methacrylate derivatives.⁹ Since 1,1-diethylsilabutane (SB) is a typical nonpolar segment and 2-hydroxyethyl methacrylate (HEMA) has high polarity, the block copolymer having both segments is expected to behave as an amphiphile. Nakahama et al. have reported that the surface of amphiphilic copolymer films contain HEMA as a hydrophilic segment changes to hydrophilic one when it is exposed to water and reverts to hydrophobic by annealing.¹⁰ The copolymers which we present here are also expected to show interesting environment responses, i.e., a different architecture depending on the solvent polarity.

Small-angle X-ray scattering (SAXS)^{11,12} is a method to measure the angle dependence of the scattered intensity of incident rays from the sample, which allows dimensions to be measured in the range 10–500 Å. It was first applied for the micellar system of a block copolymer in a selective solvent in 1973.¹³ From the SAXS profile, we can extract information regarding the size, the shape, and the aggregation number of micelles.

In this paper, the micellar structure of amphiphilic block copolymers poly(1,1-diethylsilabutane)-*block*-poly(2-hydroxyethyl methacrylate) (poly(SB-*b*-HEMA)) in methanol and methanol/toluene mixed solvents has been studied by SAXS technique. In addition, the structures of the aggregates are quantitatively investigated and related to the polymer composition and the solvent composition.

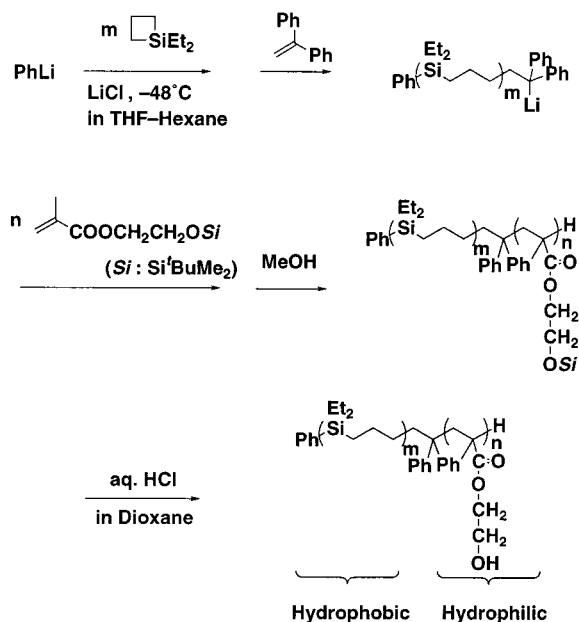
II. Experimental Section

A. Synthesis of Poly(SB-*b*-HEMA) Block Copolymers.

Two monomers (1,1-diethylsilacyclobutane and 2-(*tert*-butyldimethylsiloxy)ethyl methacrylate) and other materials used for polymerization were prepared according to the reported procedure.⁹ Purity of both monomers were checked by ¹H NMR to be >99%. Block polymerization was performed as shown in Scheme 1. To a 50 mL round-bottomed flask were introduced lithium chloride (0.35 M THF solution, 1.0 mL, 0.35 mmol), THF (5 mL), and hexane (4 mL) under an argon atmosphere. The solvents were titrated with a THF solution of lithium naphthalene to eliminate reactive impurities. A phenyllithium diethyl ether solution (1.0 M, 0.25 mL, 0.25 mmol) and 1,1-diethylsilacyclobutane were added at –48 °C and the reaction mixture was stirred for 1 h. To the solution thus prepared was added 1,1-diphenylethylene (0.088 mL, 0.50 mmol). After the solution was stirred for 30 min, 2-(*tert*-butyldimethylsiloxy)ethyl methacrylate was introduced, and the solution was stirred for another 1 h. The polymerization was terminated by addition of methanol (0.5 mL). To obtain copolymers with different block ratios, the amount of each monomer was varied.

The copolymers were hydrolyzed by diluted hydrochloric acid (3 M, 1.0 mL) in 1,4-dioxane (12 mL) at room temperature for 24 h, and led to poly(1,1-diethylsilabutane)-*block*-poly(2-

* To whom correspondence should be addressed.

Scheme 1. Synthesis of Poly(SB-*b*-HEMA)

hydroxyethyl methacrylate) block copolymers. The products were purified by dialysis with deionized water, which gave a white precipitate, and filtered out and dried in vacuo.

B. Characterization of Copolymers. Gel permeation chromatography (GPC) was carried out by a Jasco 880-PU chromatograph equipped with four polystyrene gel columns (Shodex K-802, K-803, K-804, and K-805) and a Jasco 830-RI refractive index detector. ^1H NMR spectra were obtained on a JEOL GSX 270 spectrometer. Molecular characterizations of the copolymers were performed before hydrolysis, since chloroform, which is the eluent of GPC, was not a good solvent for HEMA, while the precursor polymers were molecularly dissolved in chloroform. In addition, we confirmed by ^1H NMR that no subreaction had taken place during hydrolysis, such as polymer degradation process.

C. Small-Angle X-ray Scattering (SAXS). The SAXS measurements were performed using a Kratky type camera (Rigaku Corp., Tokyo) equipped with a rotating anode X-ray generator and a position sensitive proportional counter (PSPC). The SAXS instrument has been described in detail elsewhere.¹⁴

Methanol and toluene (extra pure grade) were used without further purification. Methanol/toluene solvent mixtures with different mixing ratios in volume were prepared. Polymer solutions were prepared by direct dissolution of the copolymer into methanol or solvent mixtures. In all cases, the polymer concentration was 1 wt % and measurement was performed at room temperature. Sample solutions were measured in glass capillaries (Mark, Berlin) with a diameter of 2 mm. In experimental data, the scattering intensity of corresponding solvent has been subtracted.

D. Fitting Procedure of SAXS Data. Neglecting interparticle scattering contributions, the scattering intensity $I(q)$ of a particle of spherically symmetrical is proportional to the square of the structure amplitude $F(q)$, which is obtained by the Fourier transform of the electron density distribution function $\rho(r)$.

$$I(q) \propto \{F(q)\}^2 \quad (1)$$

$$F(q) = 4\pi \int_0^\infty \rho(r) r^2 \sin(qr)/(qr) dr \quad (2)$$

The scattering vector q is given by $q = 4\pi(\sin \theta)/\lambda$, where 2θ is the scattering angle and λ is the X-ray wavelength.

Since methanol is a good solvent for HEMA and a poor solvent for SB, the block copolymers are expected to form micelles in methanol consisting of a core composed of SB and

a shell of HEMA swollen by the solvent. For the micelles in methanol, we applied several models to fit the SAXS data.

1. Simple Core-Shell Model. When the micelles are assumed to consist of spherical core-shell structure with no spatial variation of the electron density in the core and the shell regions, the scattering amplitude of eq 2 can be given as follows:¹¹

$$F(q) = (\rho_C - \rho_S) V_C \Phi_C(q) + (\rho_S - \rho_0) V_S \Phi_S(q) \quad (3)$$

$$\Phi_C(q) = 3(\sin(qR_C) - qR_C \cos(qR_C))/(qR_C)^3 \quad (4)$$

$$\Phi_S(q) = 3(\sin(qR_S) - qR_S \cos(qR_S))/(qR_S)^3 \quad (5)$$

R_C and R_S denote the radii of the core and the overall micelle, ρ_C , ρ_S , ρ_0 the electron densities of the core, the shell, and the solvent, and V_C and V_S the volumes of the core and the overall micelle, respectively. Using the calculable values of the electron densities of the monomer units (ρ_{SB} and ρ_{HEMA}) and the solvent (ρ_0), ρ_C and ρ_S are given by

$$\rho_C = \rho_{\text{SB}} \quad (6)$$

$$\rho_S = \phi_{\text{Sol}} \rho_0 + (1 - \phi_{\text{Sol}}) \rho_{\text{HEMA}} \quad (7)$$

where ϕ_{Sol} is the volume fraction of the solvent in the shell, which can be calculated by the following equation with the degree of polymerization of HEMA (n) and the volume of HEMA repeat units (v_{HEMA}):

$$\phi_{\text{Sol}} = 1 - \phi_{\text{HEMA}} = 1 - N_{\text{agg}} n v_{\text{HEMA}} / (V_S - V_C) \quad (8)$$

Here ϕ_{HEMA} is the volume fraction of HEMA in the shell. N_{agg} denotes the aggregation number of the micelles, which is calculated from V_C , the degree of polymerization of SB (m), and the volume of SB repeat units (v_{SB}):

$$N_{\text{agg}} = V_C / (m v_{\text{SB}}) \quad (9)$$

Assuming that the critical micelle concentration is negligibly low, i.e., all polymers contribute to the micelle formation, the number density n_p of the micelles is then calculated as

$$n_p = \phi / (N_{\text{agg}} (m v_{\text{SB}} + n v_{\text{HEMA}})) \quad (10)$$

where ϕ is the volume fraction of copolymer in solution. The scattering intensity is finally given by the product of the form factor and the number density of the micelles. However, we introduced a shift factor, f , since the intensity of the experimental data is obtained in arbitrary units because the data have not been calibrated to an absolute scale.

$$I(q) = f n_p \{F(q)\}^2 \quad (11)$$

The values of $\rho_{\text{SB}} = 0.280$, $\rho_{\text{HEMA}} = 0.396$, and $\rho_0 = 0.268 \text{ \AA}^{-3}$ were fixed, and three parameters, R_C , R_S , and f , were variables in the fitting procedure, while the value of f was arranged to be the same for all data.

2. Core-Corona Model (Star Model). In this model we adapt the Daoud-Cotton treatment¹⁵ of star polymers to treat micellar coronas, that is, the volume fraction of HEMA in the shell (ϕ_{HEMA}) is assumed as a decreasing function of r , where r is the distance from the micelle center. First we assume that $\phi_{\text{HEMA}}(r)$ decays as r^{-b} :

$$\phi_{\text{HEMA}}(r) = a(r/R_C)^{-b} \quad \text{for } R_C < r < R_S$$

$$\phi_{\text{HEMA}}(r) = 0 \quad \text{for } R_S < r \quad (12)$$

a is the volume fraction of HEMA at the core-shell interface. The electron density of shell is also a function of r :

$$\rho_S(r) = \phi_{\text{HEMA}}(r) \rho_{\text{HEMA}} + (1 - \phi_{\text{HEMA}}(r)) \rho_0 \quad (13)$$

Table 1. Characterization of Poly(SB-*b*-HEMA)

polymer	$m_0/i_0 \cdot n_0/i_0^a$	$m:n^b$	M_w/M_n^c
A	20:20	26:24	1.20
B	10:20	12:22	1.20
C	10:30	13:37	1.28

^a The initial molar ratios of [1,1-diethylsilacyclobutane]/[phenyllithium] and [2-(*tert*-butyldimethylsiloxy)ethyl methacrylate]/[phenyllithium]. ^b Obtained by ¹H NMR before hydrolysis. ^c By GPC before hydrolysis.

the scattering amplitude is

$$F(q) = (\rho_C - \rho_0) V_C \Phi_C(q) + 4\pi \int_{R_C}^{R_S} (\rho_S(r) - \rho_0) r^2 \sin(qr)/(qr) dr \quad (14)$$

R_S can be obtained as the value satisfying the following equation:

$$4\pi \int_{R_C}^{R_S} \phi_{\text{HEMA}}(r) r^2 dr = N_{\text{agg}} n V_{\text{HEMA}} \quad (15)$$

Equations 9–11 can be used for this model as well. On fitting with eq 14, the same values of R_C and f were used as obtained by the core–shell model. Then a is the only parameter as b is assigned.

3. Size Distribution. Taking the polydispersity in micelle size into account, the average scattering intensity is given by

$$I(q) = f n_p \int_0^\infty P(R) \{F(q)\}^2 dR \quad (16)$$

We assume the size distribution is given by a Gaussian function $P(R)$

$$P(R) = (2\pi)^{-1/2} \sigma_{R_S}^{-1} \exp[-(R - R_S)^2/2\sigma_{R_S}^2] \quad (17)$$

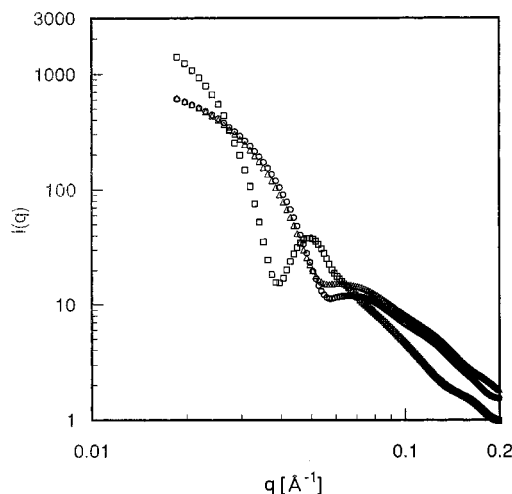
where R_S and σ_{R_S} are the average and the standard deviation of micellar size, respectively.

III. Results and Discussion

A. Characterization of Copolymers. Three copolymers with different compositions were prepared by changing the monomer/initiator ratio on polymerization, whose characteristics are tabulated in Table 1. The number-averaged degree of polymerization of SB (m) and HEMA (n) were determined by ¹H NMR, and the polydispersity indices (M_w/M_n) were determined by GPC using polystyrene as calibration standards, where M_w and M_n are the weight- and number-averaged molecular weights, respectively. The values of M_w/M_n were rather large compared with that of silabutane homopolymer (~1.09), suggesting that the polymerization of the second monomer did not proceed in a living manner. Polymer A has nearly the same length of polar segment as and a longer nonpolar segment than polymer B, and polymer C has the same value of m and a larger n than polymer B. Thus, polymer A is the copolymer with the highest hydrophobicity.

These copolymers were soluble in methanol, although silabutane homopolymer did not dissolve in methanol, which suggests an amphiphilic nature for these copolymers. Polymer A was soluble in toluene as well, but the others did not dissolve in toluene because of the shorter nonpolar segment.

B. Micelle Formation in Methanol. Since methanol is a good solvent for HEMA and a poor solvent for SB, the block copolymers are expected to form micelles in methanol consisting of a core composed of SB and a shell of HEMA swollen by the solvent. SAXS profiles of the

**Figure 1.** SAXS profiles of poly(SB-*b*-HEMA) in methanol.

copolymers in methanol are shown in Figure 1. Strong scattering at small angles is observed in all cases, suggesting the micelle formation indeed. In addition, the scattering curves exhibit a well-marked secondary maximum, indicating a well-defined structure of micelles.

First, we performed the fitting of the SAXS profile of polymer A with the theoretical curve of the simple core–shell model, and obtained good agreement at small angles ($q < 0.03 \text{ \AA}^{-1}$) and secondary maximum ($q \sim 0.05 \text{ \AA}^{-1}$). However, at minimum ($q \sim 0.04 \text{ \AA}^{-1}$) and larger q regions ($q > 0.06 \text{ \AA}^{-1}$), the intensity of the theoretical curve was lower than that of the experimental one. In addition, it is more reasonable that the polymer concentration in the shell decreases with an increase in the distance from the core surface. Hence, we tried to fit the data using the models in which the decreasing functions of the electron density profile in the shell were introduced. Figure 2 shows the fitting results with the core–corona model. In this model, ρ_S is assumed to decrease as r^{-b} . The value of b was changed from 0 to 2. $b = 0$ represents the simple core–shell model and $b = 4/3$ corresponds to the case of good solvent for polar segments.¹ Figure 2b is the electron density profiles corresponding to the scattering profiles shown in Figure 2a. Larger b produced lower secondary maximum and gave slightly larger value of R_S , but a smearing effect to reproduce the experimental data at $q \sim 0.04 \text{ \AA}^{-1}$ was not obtained.

We attempted another model proposed by Liu et al.¹⁶ as a “cap-and-gown” model, in which a Gaussian distribution of the polymer segments in the shell region is assumed, but no improvement in fitting quality as compared with the core–corona model was obtained.

Thus, it was not possible to account for the smearing effect at $q \sim 0.04 \text{ \AA}^{-1}$ with several models. Then we introduced the Gaussian distribution function in eq 16 for taking into account the polydispersity of micellar size. Figure 3 shows the fitting results of the SAXS curve of polymer A solution with eq 16. For the calculation of $F(q)$, the simple core–shell model was used. With an increase of the polydispersity (σ_{R_S}/R_S), the minimum at $q \sim 0.04 \text{ \AA}^{-1}$ in theoretical curve was smeared more obviously, and was in accordance with the experimental data at $\sigma_{R_S}/R_S = 0.11$. At larger angles ($q > 0.06 \text{ \AA}^{-1}$), however, the theoretical curve was lower than the experimental one. The deviation at larger angles is due to the low accuracy of the measured curves in this range,

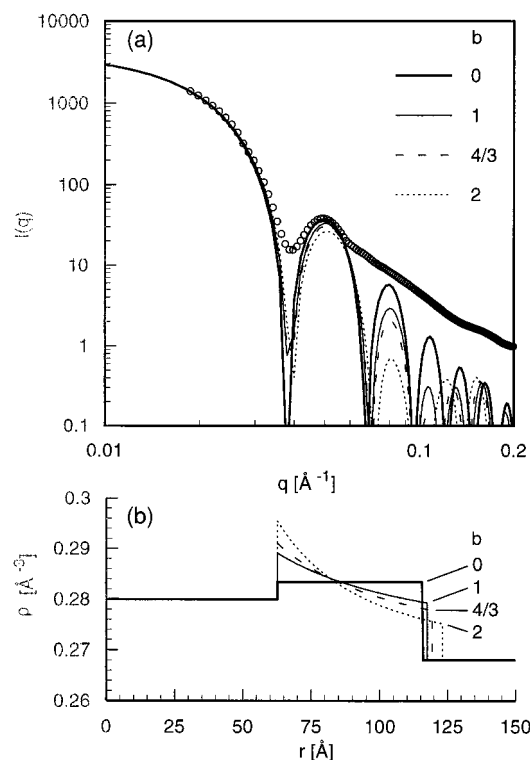


Figure 2. SAXS profile of polymer A ($m:n = 26:24$) in methanol with theoretical curves of the core-corona model. The curve $b = 0$ corresponds to the simple core-shell model.

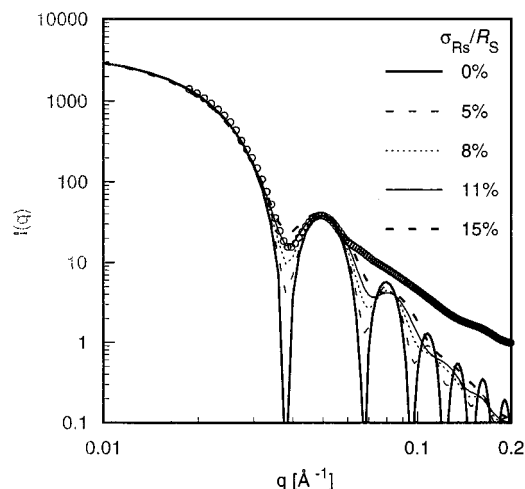


Figure 3. SAXS profiles of polymer A ($m:n = 26:24$) in methanol with theoretical curves of the simple core-shell model, taking the micellar size distribution into consideration.

and also due to the fact that the scattering at larger angles is dominated by individual fluctuation of polymer chains in the shell (blobs),¹⁷ which was not considered in the present model. However, it can be concluded that the simple core-shell model with the size distribution adequately described the experimental data, and the variation of the polymer concentration in the corona region did not necessarily have to be considered.

C. Dependence of Micelle Size on Polymer Composition. The SAXS curves were well reproduced by the theoretical curves of the simple core-shell model as shown in Figure 4 with the parameters listed in Table 2. To obtain better agreement between experimental and theoretical curves, Gaussian type distribution function of micelle size was introduced as described above.

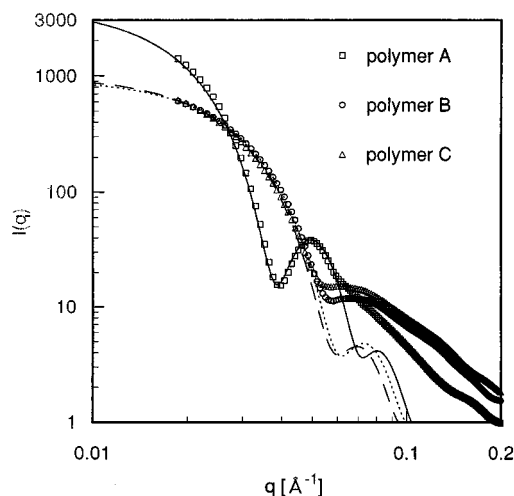


Figure 4. SAXS profiles of poly(SB-*b*-HEMA) in methanol. Solid, dotted, and broken lines are theoretical curves of the simple core-shell model for polymers A, B, and C, respectively.

Table 2. Fitting Results of SAXS Curves of Micelles in Methanol

polymer	$m:n$	R_C (Å) ^a	R_S (Å) ^b	N_{agg} ^c	σ_{R_S}/R_S ^d	ϕ_{Sol} ^e
A	26:24	63	108	154	0.11	0.85
B	12:22	30	73	35	0.12	0.91
C	13:37	25	76	20	0.12	0.93

^a The radius of the core. ^b The radius of the overall micelle. ^c The aggregation number. ^d The polydispersity of the overall micellar size. ^e The volume fraction of the solvent in the shell.

The resultant value of the polydispersity (σ_{R_S}/R_S) was 11–12% in all cases. From Table 2, one can qualitatively understand the relationship between polymer composition and micellar structure. Increase of SB chain length (m) or reduction of HEMA length (n) enhances the aggregation number (and R_C also). On the other hand, total micellar size (R_S) is almost independent of n , which is found by comparison between polymer B and C.

D. Relationship between Polymer Morphology and Solvent Composition. Toluene is a good solvent for SB and poor solvent for HEMA, in contrast with methanol. Since methanol and toluene are miscible with each other, the effect of solvent selectivity on polymer morphology can be investigated by utilization of a methanol/toluene mixed solvent with changing its mixing ratio. Polymer A was used for this purpose, because polymers B and C were not soluble in toluene, which produced a turbid suspension with a small amount of precipitate due to the shorter nonpolar chain. Seven solvent mixtures of different mixing ratios and two pure solvents (methanol:toluene = 8:0, 7:1, 6:2, 5:3, 4:4, 3:5, 2:6, 1:7, 0:8) were prepared. SAXS profiles of polymer A in these solvents are shown in Figures 5–7. The scattering profile clearly depends on the mixing ratio. With increase of the volume fraction of toluene, the intensity at small angles decreases and secondary maximum shifts to a larger q and becomes broader first (Figure 5), then the intensity increases again when the amount of toluene exceeds that of methanol. However, the secondary maximum is not observed (Figures 6 and 7). The morphology of the copolymer in the solutions studied here can be classified into three regimes.

1. Micelle Region (Methanol:Toluene = 8:0, 7:1, 6:2, 5:3). The solutions under methanol-rich conditions show SAXS profiles similar to that in pure methanol, providing a clear secondary maximum peak as shown

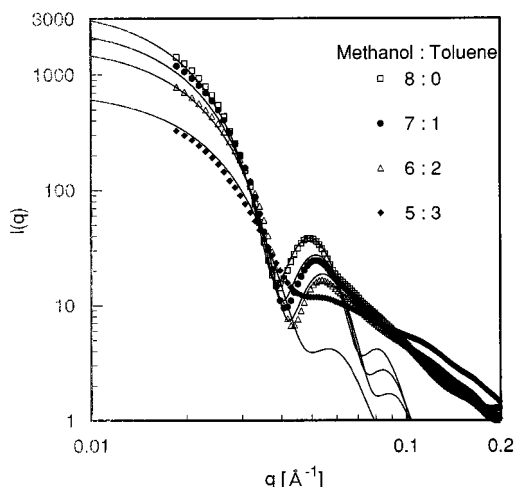


Figure 5. SAXS profiles of polymer A ($m:n = 26:24$) in methanol/toluene solvent mixtures. The polymers are suggested to form micelles under methanol-rich conditions.

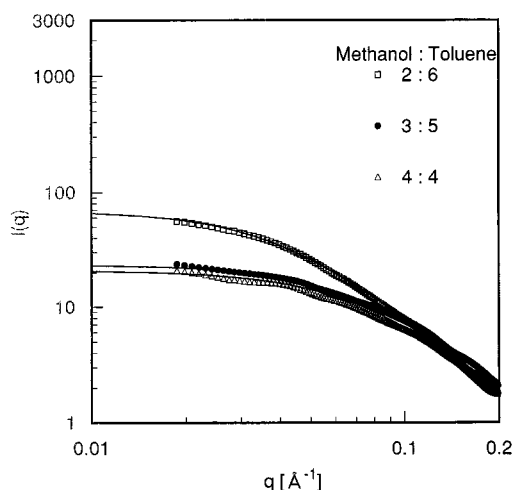


Figure 6. SAXS profiles of polymer A ($m:n = 26:24$) in methanol/toluene solvent mixtures. The polymers are suggested to exist in an unimer state at intermediate mixing ratios.

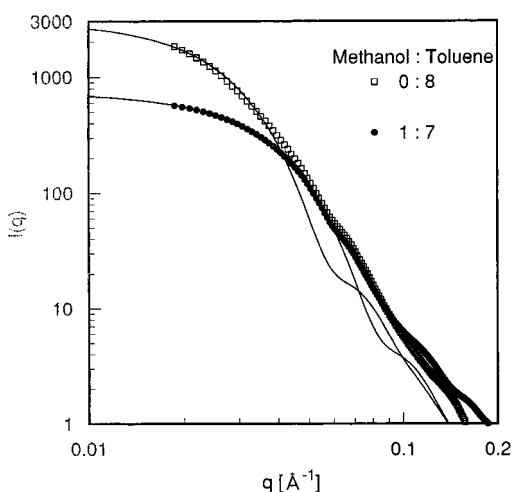


Figure 7. SAXS profiles of polymer A ($m:n = 26:24$) in methanol/toluene solvent mixtures. The polymers are suggested to form reversed micelles under toluene-rich conditions.

in Figure 5. These profiles suggest the micelle formation, and were fitted by theoretical curves of a core-shell model assuming a solid core composed by pure SB

and a solvent-swollen shell of HEMA. The fitting curves are shown by lines in Figure 5. The fitting curves convoluted the distribution function of R_S as described above. The scattering at smaller angles and the secondary maximum are well reproduced by fitting curves. Only the case of methanol:toluene = 5:3, could the height of the secondary maximum not coincide with the fitting curve, which is probably due to the fact that unimers, which will be described later, also exist in the micellar solution to some extent.

2. Unimer Region (Methanol:Toluene = 4:4, 3:5, 2:6). The scattering from the solution at intermediate mixing ratios is weak and shows a monotonic decrease against q , as can be seen in Figure 6. The scattering profiles could be fitted by the Debye formula¹⁸ which is applied for Gaussian chains with the radius of gyration R_G :

$$P(q) = 2\{x - 1 + \exp(-x)\}/x^2 \quad (18)$$

$$x = q^2 R_G^2 \quad (19)$$

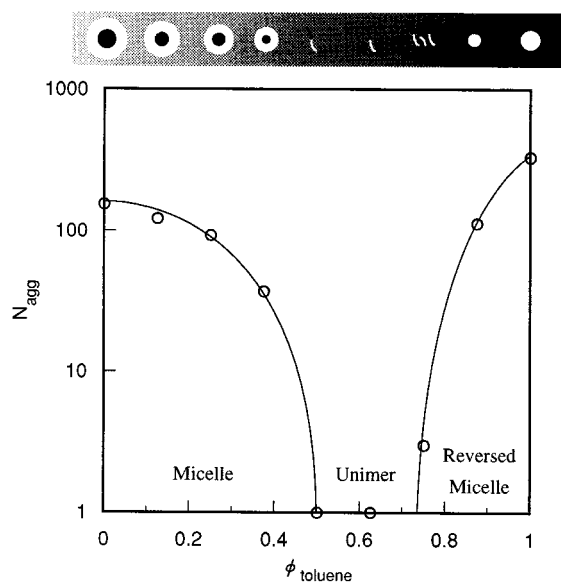
The good agreement between experimental and theoretical curves indicates that the polymers exist in an unimer state in these solutions. Obtained R_G values were small enough for 4:4 (22 Å) and 3:5 solutions (23 Å), which also suggests the unimer state. In the case of 2:6 solution, however, both the scattering intensity at smaller angles and the radius of gyration (40 Å) were larger than the others, implying a possibility of the formation of small aggregates. If the aggregation number is assumed to be proportional to the forward scattering intensity, it can be approximately calculated to be 3 by comparison with the 3:5 solution in which the polymers were thought to exist as unimers.

3. Reversed Micelle¹⁹ Region (Methanol:Toluene = 1:7, 0:8). Under toluene-rich conditions, the copolymers can be assumed to form reversed micelles, since the strong scattering was observed at smaller angles as shown in Figure 7 and the scattering profile could not be fitted by Debye function. In these conditions, the electron density of SB ($\rho_{SB} = 0.280 \text{ Å}^{-3}$) is almost identical to that of solvent ($\rho_0 = 0.281$ and 0.283 for 1:7 and 0:8, respectively); then the swollen shell of SB is "invisible", and only the core composed by HEMA is observed by X-ray. It should be noticed that the scattering intensity at wider angles obeys the Porod law;²⁰ i.e., it follows the power law of q^{-4} . This relation is satisfied if the boundary between the scattering objects and the matrix is sharp and smooth. Hence this observation means that the micelle has a sharp and smooth interface between the core and the shell, since only the core is observed in these conditions. Assuming $\rho_S = \rho_0$ and $\rho_C = \rho_{HEMA}$ in eq 3, the scattering data were fitted by the form factor of the homogeneous isolated sphere, and here the distribution function of R_C was convoluted by replacement of R_S with R_C in eq 19. The aggregation number was given by $V_C/(nV_{HEMA})$ instead of eq 9. The fitting curves are also shown in Figure 7. The good agreement with experimental data was observed at smaller angles. However, a small discrepancy arises at larger angles where a "shoulder" is observed in theoretical curves despite high polydispersity introduced ($\sigma_{R_S}/R_S \sim 20\%$) to smear the secondary maximum. It is probably due to the oversimplification of the model. It may indicate the formation of anisotropic micelles, which will be mentioned below. However, we have not performed precise fitting using complicated models.

Table 3. SAXS Results of Polymer A in a Methanol/Toluene Mixture

ϕ_{toluene}^a	shape	R_C (Å)	R_S (Å)	R_G (Å)	N_{agg}	ϕ_{Sol}
0	micelle ^b	63	108		154	0.85
0.125	micelle ^b	58	103		122	0.86
0.25	micelle ^b	53	98		93	0.88
0.375	micelle ^b	39	89		37	0.94
0.5	unimer ^c			22	1	
0.625	unimer ^c			23	1	
0.75	unimer ^c			40	3	
0.875	reversed micelle ^d	48			113	
1	reversed micelle ^d	69			332	

^a The volume fraction of methanol in solvent. ^b SAXS data was fitted by core-shell model with parameters R_C and R_S . ^c SAXS data was fitted by Debye function with a parameter R_G . ^d SAXS data was fitted by homogeneous sphere model with a parameter R_C .

**Figure 8.** Aggregation number of polymer A ($m:n = 26:24$) as a function of the volume fraction of toluene in solvent.

All the fitting results are shown in Table 3. The obtained aggregation number was plotted against the volume fraction of toluene in solvent (ϕ_{toluene}) in Figure 8 with schematic representation of the aggregation style. On the plot, the aggregation number of 2:6 solution was assumed to be 3. The copolymer forms relatively large micelles in methanol ($\phi_{\text{toluene}} = 0$). With an increase of ϕ_{toluene} , the solubility of the nonpolar chain (SB) increases, and then the aggregation number decreases. At $\phi_{\text{toluene}} \sim 0.5$, no aggregate is formed since both HEMA and SB are soluble. A further increase of ϕ_{toluene} reduces the solubility of the polar chain (HEMA), induces the formation of the reversed micelles, and enhances the aggregation number. Similar behavior has been reported for the polystyrene-*b*-poly(ethylene/propylene) block copolymer in *n*-dodecane/1,4-dioxane mixtures.²¹ In pure toluene ($\phi_{\text{toluene}} = 1$), quite large aggregates are formed, and in fact, the obtained value of $R_C = 69$ Å is larger than the contour length of the HEMA block of the copolymer (60 Å). It implies the possibility of a formation of anisotropic micelles of which one or two dimensions are less than the contour length. Indeed, the scattering curve at $\phi_{\text{toluene}} = 1$ could be fitted by the theoretical curve of the prolate ellipsoid whose half-length of the minor axes corresponds to the contour length, and the ratio of major and minor axes is 3:1.

However, we cannot draw any conclusions here about the micellar shape, since the scattering profile is hardly distinguishable between ellipsoids and polydisperse spheres; moreover, making sure of the existence of large dimensional aggregates (a cylinder, for example) requires data at smaller angles than those covered in this experiment.

IV. Conclusions

Amphiphilic block polymers of poly(SB-*b*-HEMA) were synthesized by addition of 2-(*tert*-butyldimethylsiloxy)-ethyl methacrylate to a living poly(1,1-diethylsilabutane) end-capped with 1,1-diphenylethylene. SAXS measurements were performed for these copolymers in methanol and in methanol/toluene mixtures. They formed spherical micelles in methanol, whose scattering curves were well described by the simple core-shell model. The aggregation number of micelles in methanol increased with an increase of SB chain length or a reduction of HEMA, while the total micellar size (R_S) was almost independent of the degree of polymerization of HEMA. Such tendency corresponds to the previous report with other amphiphilic polymer in aqueous media.⁸ In the solvent mixtures, three different morphologies of the polymer, i.e., a continuous change from micelle to reversed micelle via unimer with increasing volume fraction of toluene, were observed.

In this way, the block copolymer synthesized in this study has been shown to be a valuable example for understanding its morphology depending on its composition and/or solvent polarity. In addition, we have found that the copolymer forms a quite stable monolayer at air/water interface, which will be described in a forthcoming paper.²²

Acknowledgment. This work was supported by Grant-in-aid of the Ministry of Education, Science, Sports and Culture of Japan (No. 09232230 and 09305062). M.N. gratefully acknowledges the support of this work by Research Fellowships of the Japan Society for the Promotion of Science for Young Scientists.

References and Notes

- Halperin, A.; Tirrell, M.; Lodge, T. P. *Adv. Polym. Sci.* **1992**, *100*, 31.
- Chu, B. *Langmuir* **1995**, *11*, 414.
- Tuzar, Z.; Kratochvil, P. *Advances in Colloid and Interface Science*; Elsevier: Amsterdam, 1976.
- Zana, R. *Colloid Surf. A: Physicochem. Eng. Aspects* **1997**, *123–124*, 27.
- Yamaoka, H.; Matsuoka, H.; Sumaru, K.; Hanada, S.; Imai, M.; Wignall, G. D. *Physica B* **1995**, *213&214*, 700.
- Nakano, M.; Yamaoka, H.; Poppe, A.; Richter, D. *Physica B* **1998**, *241–243*, 1038.
- Nakano, M.; Matsuoka, H.; Yamaoka, H.; Poppe, A.; Richter, D. *Macromolecules* **1999**, *32*, 697.
- Nakano, M.; Matsumoto, K.; Matsuoka, H.; Yamaoka, H. *Macromolecules* **1999**, *32*, 4023.
- Matsumoto, K.; Deguchi, M.; Nakano, M.; Yamaoka, H. *J. Polym. Sci., Part A: Polym. Chem.* **1998**, *36*, 2699.
- Senshu, K.; Yamashita, S.; Ito, M.; Hirao, A.; Nakahama, S. *Langmuir* **1995**, *11*, 2293.
- Guinier, A.; Fournet, G. *Small-Angle Scattering of X-rays*; John Wiley: New York, 1955.
- Glatzer, O.; Kratky, O. *Small-Angle X-ray Scattering*; Academic Press: London, 1982.

- (13) Pleštil, J.; Baldrian, J.; *Macromol. Chem.* **1973**, 174, 183.
- (14) Ise, N.; Okubo, T.; Kunugi, S.; Matsuoka, H.; Yamamoto, K.; Ishii, Y. *J. Chem. Phys.* **1984**, 81, 3294.
- (15) Daoud, M.; Cotton, J. P. *J. Phys. (Paris)* **1982**, 43, 531.
- (16) Liu, Y.; Chen, S. H.; Huang, J. S. *Macromolecules* **1998**, 31, 2236.
- (17) Richter, D.; Schneiders, D.; Monkenbusch, M.; Willner, L.; Fetters, L. J.; Huang, J. S.; Lin, M.; Mortensen, K.; Farago, B. *Macromolecules* **1997**, 30, 1053.
- (18) Debye, P. *J. Chem. Phys.* **1946**, 14, 636.
- (19) We use the term "reversed micelle" to indicate the aggregate formed in nonpolar solvent, while "micelle" is used when the aggregates are formed in polar solvent.
- (20) Porod, G. *Kolloid-Z.* **1951**, 124, 83.
- (21) Quintana, J. R.; Villacampa, M.; Katime, I. A. *Macromolecules* **1993**, 26, 601.
- (22) Nakano, M.; Deguchi, M.; Endo, H.; Matsumoto, K.; Matsuoka, H.; Yamaoka, H. *Macromolecules* **1999**, 32, 6088.

MA981912C